

Excitation of ^{229m}Th at Inelastic Scattering of Low Energy Electrons.

E. V. Tkalya^{1,2,3,*}

¹*P.N. Lebedev Physical Institute of the Russian Academy of Sciences, 119991, 53 Leninskiy pr., Moscow, Russia*

²*National Research Nuclear University MEPhI, 115409, Kashirskoe shosse 31, Moscow, Russia*

³*Nuclear Safety Institute of RAS, Bol'shaya Tulsкая 52, Moscow 115191, Russia*

(Dated: July 24, 2020)

Excitation of the anomalously low lying nuclear isomer $^{229m}\text{Th}(3/2^+, 8.28 \pm 0.17 \text{ eV})$ in the process of inelastic electron scattering is studied theoretically in the framework of the perturbation theory for the quantum electrodynamics. The calculated cross sections of ^{229m}Th by the extremely low energy electrons in the range 9 eV–12 eV for the Th atom and $\text{Th}^{1+,4+}$ ions lie in the range 10^{-25} – 10^{-26} cm^2 . Being so large, the cross section opens up new possibilities for the effective non-resonant excitation of ^{229m}Th in experiments with an electron beam or electron (electric) current. This can be crucial, since the energy of the isomeric state is currently known with an accuracy insufficient for the resonant excitation by photons. In addition, the cross section of the time reversed process is also large, and as a consequence, the probability of the non-radiative ^{229m}Th decay via the conduction electrons in metal is $\approx 10^6 \text{ s}^{-1}$, that is, close to the internal conversion probability in the Th atom.

PACS numbers: 25.30.Dh, 27.90.+b

Over the past 30 years the anomalously low-lying isomeric level $3/2^+(E_{\text{is}} < 10 \text{ eV})$ in the ^{229}Th nucleus has been the subject of intensive study in experimental and theoretical ways. Being recently adopted, the value for the energy of the isomeric state, $E_{\text{is}} = 8.28 \pm 0.17 \text{ eV}$, was obtained in Ref. [1]. This result was preceded by a long period of measurements. During this time the values of $E_{\text{is}} \leq 100 \text{ eV}$ [2], $1 \pm 4 \text{ eV}$ [3], $3.5 \pm 1 \text{ eV}$ [4], and $7.8 \pm 0.5 \text{ eV}$ [5] were obtained. The present value is not the end of the story and a more refined accuracy is required for the most important applications of the Thorium isomer, namely, the nuclear clock [6–9] and the nuclear laser [10, 11].

Studies of the $^{229m}\text{Th}(3/2^+, 8.28 \pm 0.17 \text{ eV})$ isomer are also important for many others reasons, including the fundamental ones. In this paper we refer to the relative effects of the variation of the fine structure constant and the strong interaction parameter [12–14], control of the isomeric level γ decay via the boundary conditions [15] or chemical environment [16, 17], the checking of exponentiality of the decay law at long times [18], the detection of the unusual decay of the ^{229}Th ground state into the isomeric level in the muonic atom of ^{229}Th [19], the coherent oscillations between the components of the hyperfine structure in the Hydrogen-like ion $^{229}\text{Th}^{89+}$ [20], acceleration of the alpha decay of the ^{229}Th nucleus via the isomeric state [21], and so on.

The present work is focused on the excitation of the ^{229m}Th nuclear isomer, which remains one of the problems to be solved. Excitation of ^{229m}Th by laser radiation through the electron shell at the electron bridge process [22–28] is considered now as the most promising scheme to work with the ^{229}Th nucleus. Theoretically, under the resonant conditions this process provides for the efficient excitation of ^{229}Th nuclei. Unfortunately, at present it is extremely difficult to satisfy these conditions, since not

only the nuclear transition energy, but also the energies and quantum numbers of the excited states of the Th atom and ions are known with insufficient accuracy.

In this paper, the excitation of ^{229m}Th by the low energy electrons in the Thorium atom and $\text{Th}^{1+,4+}$ ions is investigated through the inelastic electron scattering. The ^{229}Th nucleus is screened by the atomic shell consisting of 90 electrons. Therefore, the main scattering channel of low energy electrons should be caused by the electron shell of the Th atom. For example, the cross section of electron impact ionization for the Th atom in the electron energy range of 10–50 eV and the total elastic scattering cross section in the range 100–200 eV reach the value of 10^{-15} cm^2 [29, 30]. Nevertheless, even in this case, the scattered electron can interact with the nucleus inelastically, since its wave function near the nucleus has a non-zero amplitude. Note, that the wave function of the low energy electron, emitted from the valence shell of the Th atom in the internal conversion process, has similar properties. (The internal conversion is the main decay channel of the ^{229m}Th isomer in the Th atom [31–34].) In the ^{229m}Th decay, the excitation energy transfers from the nucleus to the valence electron because both electron wave functions — the bound state and the continuous spectrum state — have non-zero amplitudes near the nucleus. The same holds true for scattering, with the only difference being that both wave functions belong to a continuum.

The inelastic electron scattering is not resonant. In this point, it compares favorably with the photon excitation of the ^{229}Th nucleus especially at early stages of research, with the exact value of E_{is} remaining unknown.

The cross section of the inelastic electron scattering from a nucleus is described by the second-order Feynman diagram shown in Fig. 1 and in the general case can be

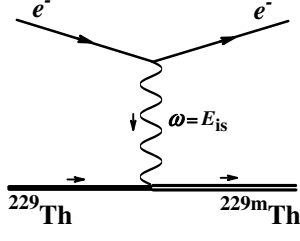


Figure 1: The Feynman diagram of the $^{229}\text{Th}(e^-, e^-)^{229m}\text{Th}$ process.

written using the Fermi golden rule,

$$\sigma = 2\pi \int d\Omega_{\mathbf{p}_f} \frac{|\langle f | H_{\text{int}} | i \rangle|^2}{v_i} \rho_f, \quad (1)$$

where $v_i = p_i/E_i$ is the speed of the scattering electron, $p_{i,f}$ and $E_{i,f} = \sqrt{p_{i,f}^2 + m_e^2}$ are the momentum and energy of the electron with mass m_e in the initial, i , and final, f , states (the system of units is $\hbar = c = 1$), $\rho_f = p_f E_f / (2\pi)^3$ is the density of final states.

The Hamiltonian of the interacting electron $j_{fi}^e(\mathbf{r})$ and nuclear $J_{fi}^s(\mathbf{R})$ currents has the form

$$\langle f | H_{\text{int}} | i \rangle = \int d^3r d^3R j_{fi}^e(\mathbf{r}) D_{\text{qs}}(\omega, \mathbf{r} - \mathbf{R}) J_{fi}^s(\mathbf{R}). \quad (2)$$

Here the photon propagator in the frequency-coordinate representation is [35] $D_{\text{qs}}(\omega, \mathbf{r} - \mathbf{R}) = -g_{\text{qs}} \exp(i\omega|\mathbf{r} - \mathbf{R}|)/|\mathbf{r} - \mathbf{R}|$, where g_{qs} is the metric tensor, $\omega = E_i - E_f$ is the energy transferred from the electron to the nucleus. This energy is equal to the isomeric state energy, i.e. $\omega = E_{\text{is}}$.

Taking into account the Siegert's theorem (see, for example, [36]) and the long-wave approximation for the photon-nucleus interaction, one can simplify the Hamiltonian in Eq. (2) by expanding it in the series over the electric, EL , and magnetic, ML , multipoles

$$\langle f | H_{\text{int}}^{E(M)} | i \rangle = 4\pi i \omega \sum_{LM} \int d^3r d^3R \mathbf{j}_{fi}(\mathbf{r}) \cdot \mathcal{B}_{LM}^{E(M)}(\omega r) \times \mathcal{A}_{LM}^{E(M)}(\omega R) \cdot \mathbf{J}_{fi}(\mathbf{R}),$$

where the dot means the scalar product of the vectors, and $\mathcal{A}_{LM}^{E(M)}$ and $\mathcal{B}_{LM}^{E(M)}$ are the well-known vector potentials [36]

$$\begin{aligned} \mathcal{A}_{LM}^E(\omega R) &= \sqrt{\frac{L+1}{2L+1}} \mathbf{Y}_{LL-1,M}(\mathbf{\Omega}_{\mathbf{R}}) j_{L-1}(\omega R) - \\ &\quad \sqrt{\frac{L}{2L+1}} \mathbf{Y}_{LL+1,M}(\mathbf{\Omega}_{\mathbf{R}}) j_{L+1}(\omega R), \\ \mathcal{A}_{LM}^M(\omega R) &= \mathbf{Y}_{LL,M}(\mathbf{\Omega}_{\mathbf{R}}) j_L(\omega R). \end{aligned}$$

The potential $\mathcal{B}_{LM}^{E(M)}$ is obtained from $\mathcal{A}_{LM}^{E(M)}$ by replacing the Bessel spherical function $j_L(x)$ with the

Hankel spherical function of the first kind $h_L^{(1)}(x)$ [37], $\mathbf{Y}_{LJ;M}(\mathbf{\Omega}_{\mathbf{R}})$ is the vector spherical harmonics [38].

Using the standard parametrization, the nuclear current is written as

$$\left| \int d^3R \mathbf{J}_{fi}(\mathbf{R}) \mathcal{A}_{LM}^{E(M)}(\omega R) \right| = \frac{\omega^L}{(2L+1)!!} \sqrt{\frac{L+1}{L}} |\langle J_f M_f | \hat{\mathcal{M}}_{LM}^{E(M)} | J_i M_i \rangle|,$$

where the introduced matrix element of the nuclear current operator $\hat{\mathcal{M}}_{LM}^{E(M)}$ between the states with spins J_i and J_f is connected with the reduced probability of the nuclear $E(M)L$ transition by the relation

$$B(E(M)L; J_i \rightarrow J_f) = \frac{1}{2J_i + 1} \sum_{M_i, M_f, M} |\langle J_f M_f | \hat{\mathcal{M}}_{LM}^{E(M)} | J_i M_i \rangle|^2.$$

In the electron current

$$\mathbf{j}_{fi}(\mathbf{r}) = e \psi_{\mathbf{p}_f \mu_f}^{(-)} \boldsymbol{\alpha} \psi_{\mathbf{p}_i \mu_i}^{(+)},$$

e is the electron charge, $\boldsymbol{\alpha} = \gamma^0 \boldsymbol{\gamma}$, and γ^i $\{i = 0, 1, 2, 3\}$ are the Dirac matrices, $\psi_{\mathbf{p}_i \mu_i}^{(+)}$ denotes the wave function of the initial state of the electron with the momentum \mathbf{p}_i and the projection of the electron spin μ_i on the direction $\boldsymbol{\nu}_i = \mathbf{p}_i/p_i$, and $\psi_{\mathbf{p}_f \mu_f}^{(-)}$ is wave function of the final state with the momentum \mathbf{p}_f and the projection μ_f of the spin on the direction $\boldsymbol{\nu}_f = \mathbf{p}_f/p_f$. These wave functions are the exact solutions of the Dirac equations which asymptotically go over into a superposition of a plane wave with a diverging and converging spherical wave [35]. The explicit form of $\psi_{\mathbf{p}\mu}^{(\pm)}$ is as follows

$$\psi_{\mathbf{p}\mu}^{(\pm)} = 4\pi \sum_{j,l,m} \psi_{E,j,l,m}(x) (\Omega_{jlm}^*(\boldsymbol{\nu}) v^\mu(\boldsymbol{\nu})) e^{(\pm)i\delta_{lj}}, \quad (3)$$

where $x = r/a_B$, a_B is the Bohr radius, j and l are the total and orbital angular momenta of the electron, m is the projection of j onto the quantization axis. The functions $\psi_{E,j,l,m}(x)$ in Eq. (3) are

$$\psi_{E,j,l,m}(x) = \frac{1}{pa_B} \sqrt{\frac{E+m_e}{2E}} \begin{pmatrix} g_{lj}(x) \Omega_{jlm}(\mathbf{r}) \\ -i f_{l'j}(x) \Omega_{jl'm}(\mathbf{r}) \end{pmatrix},$$

and $l' = 2j - l$. The large g_{lj} and small $f_{l'j}$ components of $\psi_{E,j,l,m}(x)$ are the numerical solutions of the Dirac equations for the electron energies $E > m_e$

$$\begin{aligned} g'(x) + \frac{1+\kappa}{x} g(x) - \frac{1}{e^2} \left(\frac{E}{m_e} + 1 - \frac{V(x)}{m_e} \right) f(x) &= 0, \\ f'(x) + \frac{1-\kappa}{x} f(x) + \frac{1}{e^2} \left(\frac{E}{m_e} - 1 - \frac{V(x)}{m_e} \right) g(x) &= 0. \end{aligned} \quad (4)$$

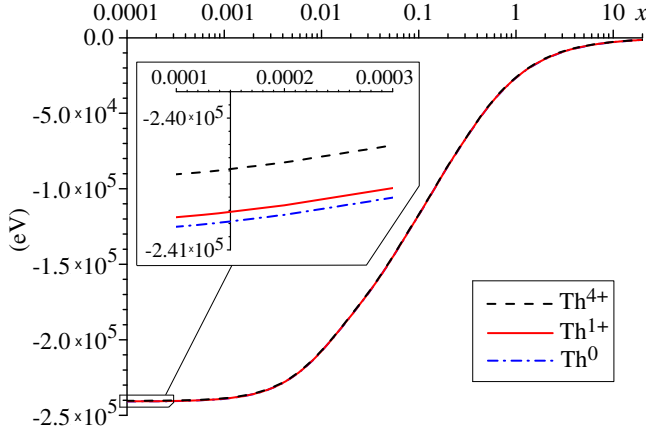


Figure 2: The electron shell potential for the Th atom and the $\text{Th}^{1+,4+}$ ions.

The functions $g_{i,f}(x)$ in Eq. (4) are normalized at $x \rightarrow \infty$ with the condition $g(x) = \sin(pa_Bx + \varphi_{lj})/x$, where φ_{lj} is a phase, $\kappa = l(l+1) - j(j+1) - 1/4$.

The potential energy $V(x)$ of the electron in Eq. 4 is the sum of the electron shell potential energy $V_{\text{shell}}(x)$ and that of the unscreened nucleus $V_{\text{nuc}}(x)$. Under the standard assumption that a nucleus with the atomic number A and the charge Z is represented by a uniformly charged sphere of the radius $x_{R_0} = R_0/a_B$, where $R_0 = 1.2A^{1/3}$ fm we conclude that the electron potential energy in its potential is $V_{\text{nuc}}(x) = -\mathcal{E}_0(Z/2x_{R_0})[3 - (x/x_{R_0})^2]$ for $0 \leq x \leq x_{R_0}$, and $V_{\text{nuc}}(x) = -\mathcal{E}_0Z/x$ for $x \geq x_{R_0}$ where $\mathcal{E}_0 = m_e e^4$ is the atomic unit of energy.

The electron shell potential has been found as follows. At the first stage, the electron density $\rho_e(x)$ in the Thorium atom (Th^0) and $\text{Th}^{1+,4+}$ ions (see an example in Ref. [39]) was calculated within the DFT theory [40, 41] through the self-consistent procedure. At the second stage, the radial component of the electric field as a function of x was found by the numerical integration of $\rho_e(x)$. And at the third stage, the electron shell potential was obtained by the numerical integration of the electric field. The resulting electron shell potentials for $\text{Th}^{0,1+,4+}$ are shown in Fig. 2. The potential energy $V_{\text{shell}}(x)$ for $\text{Th}^{0,1+,4+}$ is e times the corresponding functions in Fig. 2.

Substituting the expressions obtained for the currents in Eq. 1, averaging over the initial states, and summing over all final states, we arrive at the following scattering cross section,

$$\begin{aligned} \sigma = & (4\pi e)^2 a_B^2 \frac{p_f}{p_i} \frac{E_i + m}{p_i^2} \frac{E_f + m}{p_f^2} \times \\ & \sum_L \sum_{\tau=E,M} \sum_{\substack{l_i, j_i \\ l_f, j_f}} \frac{\omega^{2L+2}}{[(2L+1)!!]^2} (2j_i + 1) \times \\ & \left(C_{ji1/2L0}^{jf1/2} \right)^2 B(\tau L, J_i \rightarrow J_f) |m_{fi}^{\tau L}|^2, \end{aligned} \quad (5)$$

where $C_{ji1/2L0}^{jf1/2}$ is the Clebsch-Gordan coefficient, $m_{fi}^{\tau L}$ stands for the electron matrix elements

$$\begin{aligned} m_{fi}^{EL} &= \int_0^\infty h_L^{(1)}(\omega a_B x) [g_i(x) g_f(x) + f_i(x) f_f(x)] x^2 dx, \\ m_{fi}^{ML} &= \frac{\kappa_i + \kappa_f}{L} \int_0^\infty h_L^{(1)}(\omega a_B x) [g_i(x) f_f(x) + \\ & f_i(x) g_f(x)] x^2 dx. \end{aligned} \quad (6)$$

The summation over the orbital momenta l_i and l_f is performed in Eq. (5), since the calculation should take into account all possible combinations of angular momenta and the parity selection rules. It can be done by means of the well-known representation for the Clebsch-Gordan coefficient through the $6j$ symbol [42]

$$\left(C_{ji1/2L0}^{jf1/2} \right)^2 = (2l_i + 1)(2j_f + 1) \left(C_{li0L0}^{lf0} \right)^2 \left\{ \begin{matrix} l_i & 1/2 & j_i \\ j_f & L & l_f \end{matrix} \right\}^2.$$

We are concerned with the energy region where the kinetic energy of the electron in the initial state $E_e = E_i - m_e$ satisfies the condition $E_e \ll m_e$. In that case, the cross section (5) is simplified, taking the form

$$\begin{aligned} \sigma_{E(M)L} = & 4e^2 \lambda_{\gamma}^2 \left(\frac{E_e}{E_{\text{is}}} \right)^{-3/2} \left(\frac{E_e}{E_{\text{is}}} - 1 \right)^{-1/2} \times \\ & \frac{B(E(M)L; J_i \rightarrow J_f)}{a_B^{2L}} \times \\ & \sum_{\substack{l_i, j_i \\ l_f, j_f}} \frac{(2l_i + 1)(2j_i + 1)(2j_f + 1)}{(2L + 1)^2} \times \\ & \left(C_{li0L0}^{lf0} \right)^2 \left\{ \begin{matrix} l_i & L & l_f \\ j_f & 1/2 & j_i \end{matrix} \right\}^2 |\tilde{m}_{fi}^{E(M)L}|^2, \end{aligned} \quad (7)$$

where $\lambda_{\gamma} = 2\pi/E_{\text{is}}$ is the wavelength of the isomeric nuclear γ transition. The electron matrix elements in Eq. (7) are

$$\begin{aligned} \tilde{m}_{fi}^{EL} &= \int_0^\infty [g_i(x) g_f(x) + f_i(x) f_f(x)] \frac{dx}{x^{L-1}}, \\ \tilde{m}_{fi}^{ML} &= \frac{\kappa_i + \kappa_f}{L} \int_0^\infty [g_i(x) f_f(x) + f_i(x) g_f(x)] \frac{dx}{x^{L-1}}. \end{aligned} \quad (8)$$

In the case of the ML transition, one needs to change $l_i \rightarrow l'_i = 2j_i - l_i$ in formulas (7)–(8).

Two remarks are in order about the numerical solution of Eq. (4) and the calculation of the integrals in Eq. (6). First, the numerical solution of the Dirac Eq. (4) for the wave function of the final state reaches the asymptotic behavior very slowly near the reaction threshold at $E_e = 8.3\text{--}8.5$ eV. Here, the energy of the scattered electron is very small, and the wavelength, respectively, is large. Therefore, it is necessary to carry out calculations up to $x \approx 2 \times 10^4$ for the correct normalization

of the wave function. Second, the integrals in the matrix elements formally diverge in Eq. (6), and converge in Eq. (8). In our case, when $\omega a_B \approx 1/450$, the approximation $h_L^{(1)}(\omega a_B x) \approx -i(2L-1)!!/(\omega a_B x)^{L+1}$ [37] used to derive Eq. (8) is valid in the region $0 \leq x \lesssim 50$. Nevertheless, the use of formulas (8) is quite correct. Integration over large values of the variable, $x \geq 50$, does not lead to a divergence of the integrals in Eq. (6) due to the fast oscillations of the integrand. The characteristic “period” of these oscillations $x_{\lambda_e} = \lambda_e/a_B \leq 8$ is determined by the wavelength of the electron in the initial state. In the energy range $E_e \geq E_{is}$, the condition $\lambda_e \leq 8a_B$ is always satisfied, leading to the fast convergence of the integrals. In addition, it follows from the numerical calculation (see the Supplement) that the largest contribution (95%) to the electron matrix elements (6) and (8) is due to the integration from a much smaller area, $0 \leq x \lesssim 0.01$.

Currently, there are no experimental data on the excitation of the low-lying nuclear states by the low energy electrons. That is why the model was tested using the atomic data. The excitation cross section of the Th atom in the $7s_{1/2} \rightarrow 7p_{1/2}$ transition calculated by formula (7) is in good agreement with the similar data for the Pb atom [43] if one replaces in Eq. (7) a nuclear matrix element with the indicated atomic E1 matrix element.

The cross sections for two sets of the reduced probabilities $B_{W.u.}(M1; J_i \rightarrow J_f)$ and $B_{W.u.}(E2; J_i \rightarrow J_f)$ are shown in Fig. 3. The first set is based on the experimental data [44–47] for the M1 and E2 transitions between the rotation bands $3/2^+$ [631] and $5/2^+$ [633] in the ^{229}Th nucleus found with Alaga rules in Refs. [18, 48]). The second set utilizes $B_{W.u.}$ for the M1 and E2 transitions from Ref. [49], resulting from the computer calculation made in the compliance with the modern nuclear models.

Within the considered region of small E_e , the radial electron wave functions are proportional to $E_e^{1/4}$ in the initial state, and to $(E_e - E_{is})^{1/4}$ in the final state in the Coulomb potential [50]. As a result, for the $\text{Th}^{1+,4+}$ cross section, we obtain the dependence $\sigma \propto 1/E_e$, Fig. 3.

The difference in the shape of the cross sections for the atom and the ions near the reaction threshold of 8.28 eV is due to the fact that in case of atom the electron interacts with the nucleus at relatively short distances ($\lesssim a_B$) when it penetrates into the electron shell, whereas in the case of ions the Coulomb interaction occurs at larger distances. For the Th atom near the reaction threshold $\sigma \propto \sqrt{E_e - E_{is}}$ [50] and tends to zero at $E_e \rightarrow E_{is}$. In the case of the $^{229}\text{Th}^{1+,4+}$ ions, the cross section near the reaction threshold approaches a constant, $\sigma \rightarrow \text{const}$ [50].

As for the contributions to the cross section of partial waves, then, as one would expect [50], the S wave, namely the $S_{1/2}^{(i)} \rightarrow S_{1/2}^{(f)}$ transition, makes the largest contribution to the M1 scattering (see the Supplement),

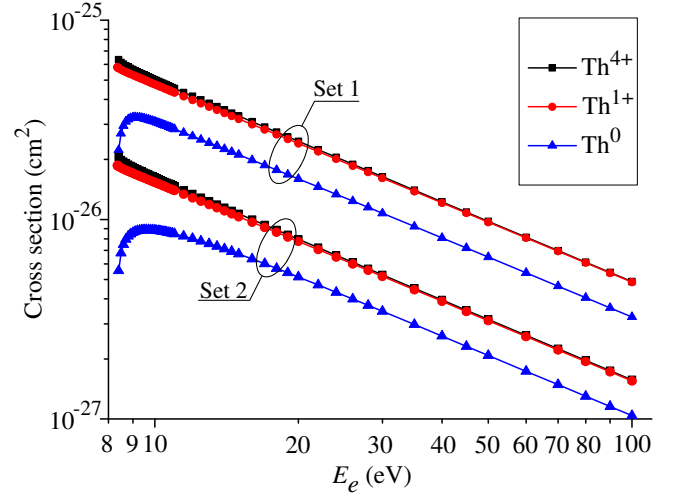


Figure 3: The electron inelastic scattering cross section of the process $^{229}\text{Th}^{0,1+,4+}(e^-, e^-)^{229m}\text{Th}^{0,1+,4+}$ with two data sets: Set 1 — $B_{W.u.}(M1, 5/2^+ \rightarrow 3/2^+) = 0.031$ and $B_{W.u.}(E2, 5/2^+ \rightarrow 3/2^+) = 11.7$, Set 2 — $B_{W.u.}(M1, 5/2^+ \rightarrow 3/2^+) = 0.0076$, $B_{W.u.}(E2, 5/2^+ \rightarrow 3/2^+) = 27$.

whereas the $P_{1/2}^{(i)} \rightarrow P_{3/2}^{(f)}$ and $P_{3/2}^{(i)} \rightarrow P_{1/2}^{(f)}$ transitions are dominant for the E2 component of the cross section (see the Supplement).

Being very large, the cross section opens up completely new possibilities for the excitation and study of the low-lying nuclear isomer ^{229m}Th . The first possibility is the excitation in the dense laser plasma with the electron temperature $T \approx E_{is}$. The ratio of the number of excited nuclei (N_{is}) to the number of nuclei in the ground state (N_{gr}) in a plasma bunch with the electron energy distribution $f(E_e)$ can be estimated as in [51]

$$N_{is}/N_{gr} \approx n_e \tau \int_{E_{is}}^{\infty} f(E_e) v(E_e) \sigma(E_e) dE_e.$$

For the electrons with the Maxwell energy distribution $f(E_e)$, the reaction rate $\langle \sigma(E_e) v(E_e) \rangle$ reaches $10^{-18} - 10^{-17} \text{ cm}^3 \text{ s}^{-1}$. In the plasma produced by the laser pulse of the duration $\tau \approx 10^{-8} - 10^{-9} \text{ s}$ on a solid target, the electron density is $n_e \approx 10^{19} - 10^{20} \text{ cm}^{-3}$. As a result, we obtain $N_{is}/N_{gr} \approx 10^{-6}$, which corresponds to the efficiency of the resonant process of nuclear excitation by electron capture (NEEC). Indeed, in the NEEC process (see for example [52–54]), the nucleus is excited resonantly by the plasma electrons with the energy of $E_{eres} \approx E_{is} - |E_b|$, where E_b is the electron binding energy for the ionized shell (for simplicity, in the Thorium atom, we consider only the shell that makes the main contribution to the probability of the internal conversion, Γ_{is}^{IC} , during the decay of ^{229m}Th). For NEEC, the working region of the electron spectrum equals approximately to the internal conversion width of the nuclear state, i.e. Γ_{is}^{IC} . The energy of resonant electrons is $E_{eres} \approx 2 \text{ eV}$, because the characteristic binding energy of the valence

electrons in Th is about 6 eV. As a consequence, the effective NEEC cross section from the electrons with the resonant wave length $\lambda_{\text{eres}} = 2\pi/\sqrt{2m_e E_{\text{eres}}}$ is

$$\sigma_{\text{NEEC}} \approx (\lambda_{\text{eres}}/2)^2 \Gamma_{\text{is}}^{\text{IC}}/T \approx 10^{-25} \text{ cm}^2$$

for the radiation width of the isomeric transition $\Gamma_{\text{is}}^{\text{rad}} \approx 3.6 \times 10^{-19} \text{ eV}$ and the internal conversion coefficient $\alpha = 1.6 \times 10^9$. Taking into account the factor $f(E_{\text{eres}})$ one can obtain the same value $N_{\text{is}}/N_{\text{gr}} \approx 10^{-6}$ for the fraction of the excited nuclei. (That is only to be expected, as, according to the perturbation theory for the quantum electrodynamics, the inelastic electron scattering and NEEC are the second-order processes described by the same Feynman diagram.) For further studies, Th ions with the ^{229}Th excited nuclei can be extracted by an external electric field from a plasma and implanted into thin film with a wide-gap dielectric material (SiO_2) (see details in Refs. [55–58]).

The second possibility is to excite ^{229m}Th by the electron (electric) current in solids or in experiments with the high-current electron beam [59]. For the density of implanted nuclei $\rho_{\text{Th}} = 10^{18}\text{--}10^{19} \text{ cm}^{-3}$, the target thickness $h = 10 \text{ nm}$ and the current $j_e = 1 \text{ A}$, the rate of electron excitation of the isomeric nuclei in solids can be estimated as

$$dN_{\text{is}}/dt \approx \rho_{\text{Th}} h j_e \approx 10^5\text{--}10^6 \text{ s}^{-1}.$$

In the electron beam experiment, the generation of an avalanche of the secondary electrons with the energies $E_e > E_{\text{is}}$ increases the efficiency of excitation of the ^{229}Th nuclei. Note that in these experiments it is not necessary to know the energy of the nuclear isomeric level E_{is} with high accuracy to tune the electron energy, since the excitation process is non-resonant.

Another interesting opportunity to observe the process discussed above is to expose the electron shell to the intense laser field after tunnel ionization [60]. In this case the electrons accelerated back to the ionized Th atom by the laser field should excite the ^{229}Th nuclei through the inelastic scattering and NEEC.

Using the principle of detailed balance [50]

$$(2J_{\text{gr}} + 1)p_i^2 \sigma_{\text{gr} \rightarrow \text{is}} = (2J_{\text{is}} + 1)p_f^2 \sigma_{\text{is} \rightarrow \text{gr}}$$

one can also calculate the cross section for the time reversed process, which is the decay of the isomeric state through the electron states in the continuum. Such a situation arises, for example, when the isomer is implanted into metal [61]. In the free electron approximation [62] the decay probability through the conduction electrons in metal is given by

$$W_{(e,e')} \approx \rho_e v_F \sigma_{fi}.$$

Here ρ_e is the density of conduction electrons, v_F is the Fermi velocity, and E_F is the Fermi energy. For the

“standard” metal [63] with $\rho_e = 6 \times 10^{22} \text{ cm}^{-3}$ and $E_F = 5.5 \text{ eV}$ we have $W_{(e,e')} \approx 10^6 \text{ s}^{-1}$ and the half-life of the ^{229m}Th isomer is about 10^{-6} s . This is comparable to the half-life of ^{229m}Th decay via the internal conversion channel [31, 34].

In conclusion, the excitation cross section of the low lying isomer in the ^{229}Th nucleus has been calculated for the inelastic scattering of the extremely low energy electrons. Firstly, the cross section turned out to be so large that the decay probability of ^{229m}Th in the process of the conversion on the conduction electrons in metal is close to the probability of the internal conversion in the Th atom. Secondly, the calculated cross section provides for the effective excitation of ^{229m}Th : a) in the dense laser plasma with the temperature $T \approx E_{\text{is}}$, b) in solids by the electron (electric) current, c) at the high-current electron beam. Thirdly, this approach is fundamentally different from the well-known photon excitation, since it is non-resonant in nature and does not require that the energy of the excited level should be known. This is especially valuable at present, when the energy of the isomeric level is known with the accuracy of several tenths of the electron volt.

This research was supported by a grant of the Russian Science Foundation (Project No 19-72-30014).

SUPPLEMENT

Electron matrix elements

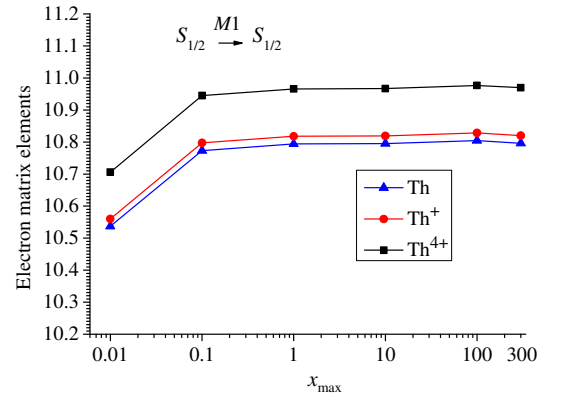


Figure 4: Electron matrix elements as a function of the end value, x_{max} , of the integral in Eq. (9).

As an example, the $M1$ electron matrix elements

$$\frac{(\omega_N a_B)^2}{3} \times (\kappa_i + \kappa_f) \int_0^{x_{\text{max}}} h_1^{(1)}(\omega a_B x) [g_i(x) f_f(x) + f_i(x) g_f(x)] x^2 dx. \quad (9)$$

for the partial $S_{1/2} \xrightarrow{M1} S_{1/2}$ transition at the energy of $E_e = 20 \text{ eV}$ are shown in Fig. 4.

Note that the matrix elements in Eq. (6) multiplied by the factor $(\omega_N a_B)^{L+1}/(2L-1)!!$ coincide with the corresponding matrix elements in Eq. (8) with the relative accuracy of 10^{-7} .

It can be seen that the matrix elements in Fig. 4 converge quickly and the main contribution to the integral comes from the region near the nucleus $0 \leq x \lesssim 0.01$.

Partial waves in cross section

The contributions of various partial waves to the $M1$ and $E2$ cross sections for the Th atom and Th^+ and Th^{4+} ions are presented in Figures 5–8.

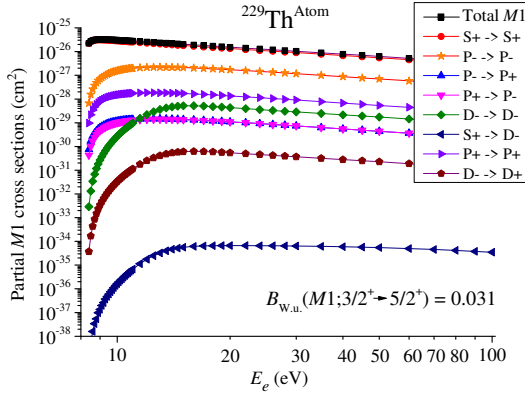


Figure 5: Partial $M1$ cross sections for the $^{229}\text{Th}(e, e')^{229m}\text{Th}$ reaction.

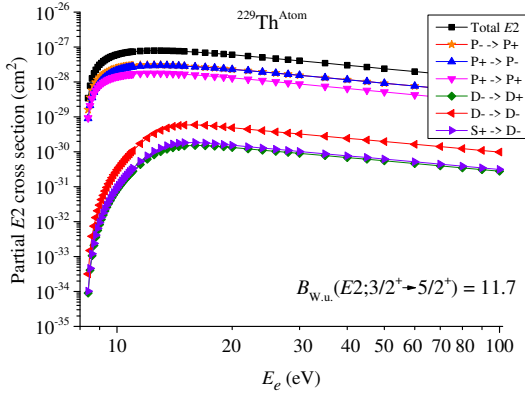


Figure 6: Partial $E2$ cross sections for the $^{229}\text{Th}(e, e')^{229m}\text{Th}$ reaction.

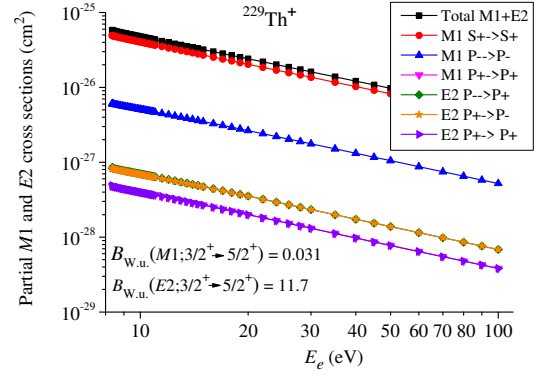


Figure 7: Partial $M1$ and $E2$ cross sections for the $^{229}\text{Th}^+(e, e')^{229m}\text{Th}^+$ reaction.

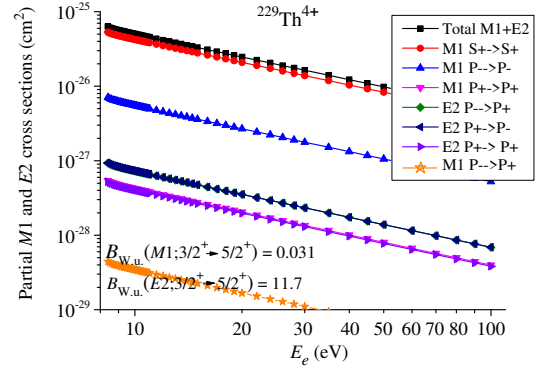


Figure 8: Partial $M1$ and $E2$ cross sections for the $^{229}\text{Th}^{4+}(e, e')^{229m}\text{Th}^{4+}$ reaction.

* Electronic address: tkalya.e@lebedev.ru

[1] B. Seiferle, L. von der Wense, P. V. Bilous, I. Amersdorfer, C. Lemell, F. Libisch, S. Stellmer, T. Schumm, C. E. Düllmann, A. Pálffy, et al., Nature **573**, 243 (2019).

- [2] L. A. Kroger and C. W. Reich, Nucl. Phys. A **259**, 29 (1976).
- [3] C. W. Reich and R. G. Helmer, Phys. Rev. Lett. **64**, 271 (1990).
- [4] R. G. Helmer and C. W. Reich, Phys. Rev. C **49**, 1845 (1994).
- [5] B. R. Beck, J. A. Becker, P. Beiersdorfer, G. V. Brown, K. J. Moody, J. B. Wilhelmy, F. S. Porter, C. A. Kilbourne, and R. L. Kelley, Phys. Rev. Lett. **98**, 142501 (2007).
- [6] E. Peik and C. Tamm, Europhys. Lett. **61**, 181 (2000).
- [7] W. G. Rellergert, D. DeMille, R. R. Greco, M. P. Hehlen, J. R. Torgerson, and E. R. Hudson, Phys. Rev. Lett. **104**, 200802 (2010).
- [8] C. J. Campbell, A. G. Radnaev, A. Kuzmich, V. A. Dzuba, V. V. Flambaum, and A. Derevianko, Phys. Rev. Lett. **108**, 120802 (2012).
- [9] E. Peik and M. Okhapkin, C. R. Phys. **16**, 516 (2015).
- [10] E. V. Tkalya, Phys. Rev. Lett. **106**, 162501 (2011).
- [11] E. V. Tkalya and L. P. Yatsenko, Laser Phys. Lett. **10**, 105808 (2013).
- [12] V. V. Flambaum, Phys. Rev. Lett. **97**, 092502 (2006).
- [13] E. Litvinova, H. Feldmeier, J. Dobaczewski, and V. Flambaum, Phys. Rev. C **79**, 064303 (2009).
- [14] J. C. Berengut, V. A. Dzuba, V. V. Flambaum, and S. G. Porsev, Phys. Rev. Lett. **102**, 210801 (2009).
- [15] E. V. Tkalya, Phys. Rev. Lett. **120**, 122501 (2018).

- [16] E. V. Tkalya, JETP Lett. **71**, 311 (2000).
- [17] E. V. Tkalya, A. N. Zherikhin, and V. I. Zhudov, Phys. Rev. C **61**, 064308 (2000).
- [18] A. M. Dykhne and E. V. Tkalya, JETP Lett. **67**, 549 (1998).
- [19] E. V. Tkalya, Phys. Rev. A **94**, 012510 (2016).
- [20] K. Pachucki, S. Wycech, J. Zylicz, and M. Pfutzner, Phys. Rev. C **64**, 064301 (2001).
- [21] A. M. Dykhne, N. V. Eremin, and E. V. Tkalya, JETP Lett. **64**, 345 (1996).
- [22] E. V. Tkalya, JETP Lett. **55**, 211 (1992).
- [23] E. V. Tkalya, Sov. J. Nucl. Phys. **55**, 1611 (1992).
- [24] P. Kalman and T. Keszthelyi, Phys. Rev. C **49**, 324 (1994).
- [25] E. V. Tkalya, V. O. Varlamov, V. V. Lomonosov, and S. A. Nikulin, Phys. Scr. **53**, 296 (1996).
- [26] S. G. Porsev, V. V. Flambaum, E. Peik, and C. Tamm, Phys. Rev. Lett. **105**, 182501 (2010).
- [27] R. A. Muller, A. V. Volotka, and A. Surzhykov, Phys. Rev. A **99**, 042517 (2019).
- [28] P. V. Borisyuk, N. N. Kolachevsky, A. V. Taichenachev, E. V. Tkalya, I. Y. Tolstikhina, and V. I. Yudin, Phys. Rev. C **100**, 044306 (2019).
- [29] T. D. Mark, Plasma Physics and Controlled Fision **34**, 2083 (1992).
- [30] R. Mayol and F. Salvat, At. Data Nucl. Data Tabl. **65**, 55 (1997).
- [31] V. F. Strizhov and E. V. Tkalya, Sov. Phys. JETP **72**, 387 (1991).
- [32] P. V. Bilous, G. A. Kazakov, I. D. Moore, T. Schumm, and A. Palffy, Phys. Rev. A **95**, 032503 (2017).
- [33] L. von der Wense, B. Seiferle, M. Laatiaoui, J. B. Neumayr, H. J. Maier, H. F. Wirth, C. Mokry, J. Runke, K. Eberhardt, C. E. Dullmann, et al., Nature **533**, 47 (2016).
- [34] B. Seiferle, L. von der Wense, and P. G. Thirolf, Phys. Rev. Lett. **118**, 042501 (2017).
- [35] V. B. Berestetskii, E. M. Lifschitz, and L. P. Pitaevskii, *Quantum Electrodynamics* (Pergamon Press, Oxford, England, 1982).
- [36] J. Eisenberg and W. Greiner, *Nuclear Theory. V. 2. Excitation Mechanisms of the Nucleus Electromagnetic and Weak Interactions* (North-Holland Publishing Company, Amsterdam-London, 1970).
- [37] M. Abramowitz and I. A. Stegun, *Handbook of Mathematical Functions* (National Bureau of Standards, Washington, D.C., 1964).
- [38] D. A. Varshalovich, A. N. Moskalev, and V. K. Khersonskii, *Quantum Theory of Angular Momentum* (World Scientific Publ., London, 1988).
- [39] E. V. Tkalya, Phys. Rev. C **100**, 054316 (2019).
- [40] A. V. Nikolaev, The FLAPW-Moscow code, Registration No. 2015616990 (Russia) from 26/06/2015.
- [41] A. V. Nikolaev, D. Lamoén, and B. Partoens, J. Chem. Phys. **145**, 014101 (2016).
- [42] A. Bohr and B. R. Mottelson, *Nuclear Structure. Vol. I: Single-Particle Motion*. (World Scientific, London, 1998).
- [43] M. P. van Eck, D. V. Fursa, I. Bray, O. Zatsarinny, and K. Bartschat, J. Phys. B: At. Mol. Opt. Phys. **53**, 015204 (2020).
- [44] C. E. Bemis, Jr., F. K. McGowan, J. L. C. Ford, Jr., W. T. Milner, R. L. Robinson, P. H. Stelson, G. A. Leander, and C. W. Reich, Phys. Scr. **38**, 657 (1988).
- [45] K. Gulda, W. Kurcewicz, A. J. Aas, M. J. G. Borge, D. G. Burkard, B. Fogelberg, I. S. Grant, E. Hagebo, N. Kaffrell, J. Kvasil, et al., Nucl. Phys. A **703**, 45 (2002).
- [46] V. Barci, G. Ardisson, G. Barci-Funel, B. Weiss, O. El Samad, and R. K. Sheline, Phys. Rev. C **68**, 034329 (2003).
- [47] E. Ruchowska, W. A. Plociennik, J. Zylicz, H. Mach, J. Kvasil, A. Algora, N. Amzal, T. Back, M. G. Borge, R. Boutami, et al., Phys. Rev. C **73**, 044326 (2006).
- [48] E. V. Tkalya, C. Schneider, J. Jeet, and E. R. Hudson, Phys. Rev. C **92**, 054324 (2015).
- [49] N. Minkov and A. Palffy, Phys. Rev. Lett. **118**, 212501 (2017).
- [50] L. D. Landau and E. M. Lifshitz, *Quantum Mechanics. Non-relativistic Theory*. (Pergamon Press, New York, 1965).
- [51] E. V. Tkalya, Laser Phys. **14**, 360 (2004).
- [52] V. I. Goldanskii and V. A. Namiot, Phys. Lett. B **62**, 393 (1976).
- [53] G. D. Doolen, Phys. Rev. Lett. **40**, 1695 (1978).
- [54] G. D. Doolen, Phys. Rev. C **18**, 2547 (1978).
- [55] V. Y. Fominiski, V. N. Nevolin, and I. Smurov, J. Appl. Phys. **96**, 2374 (2004).
- [56] P. V. Borisyuk, E. V. Chubunova, Y. Y. Lebedinskii, E. V. Tkalya, O. S. Vasiliev, V. P. Yakovlev, E. Strugovshchikov, D. Mamedov, A. Pishtshev, and S. Z. Karazhanov, Laser Phys. Lett. **15**, 056101 (2018).
- [57] P. V. Borisyuk, E. V. Chubunova, N. N. Kolachevsky, Y. Y. Lebedinskii, O. S. Vasiliev, and E. V. Tkalya, *Excitation of ^{229}Th nuclei in laser plasma: the energy and half-life of the low-lying isomeric state* (2018), 1804.00299.
- [58] Y. Y. Lebedinskii, P. V. Borisyuk, E. V. Chubunova, N. N. Kolachevsky, O. S. Vasiliev, and E. V. Tkalya, Phys. Status Solidi A **217**, 1900551 (2020).
- [59] P. V. Borisyuk, O. S. Vasilyev, Y. Y. Lebedinskii, A. V. Krasavin, E. V. Tkalya, V. I. Troyan, R. F. Habibulina, E. V. Chubunova, and V. P. Yakovlev, AIP Advances **6**, 095304 (2016).
- [60] A. V. Andreev, A. B. Savelev, S. Y. Stremoukhov, and O. A. Shoutova, Phys. Rev. A **99**, 013422 (2019).
- [61] E. V. Tkalya, JETP Lett. **70**, 371 (1999).
- [62] N. W. Aschcroft and N. D. Mermin, *Solid State Physics* (Holt, Rinehart and Winston, New York, 1976).
- [63] A. B. Pippard, Rep. Progr. Phys. **23**, 176 (1960).